

Study of ^{227}Th in the $^{226}\text{Ra}(\alpha, 3n)$ reaction

J. Manns¹, J. Gröger¹, C. Günther¹, U. Müller¹, T. Weber¹, J. de Boer²¹ Institut für Strahlen- und Kernphysik, Universität Bonn, Nussallee 14-16, D-53115 Bonn, Germany² Sektion Physik, Universität München, Am Coulombwall 1, D-85748 Garching, Germany

Received: 25 June 1998

Communicated by D.Schwalm

Abstract. The nuclear structure of ^{227}Th was studied in the $^{226}\text{Ra}(\alpha, 3n)$ reaction by gamma-ray and conversion-electron spectroscopy. Six rotational bands were identified with spins up to approximately 39/2. Attempts to connect these bands to the low-lying levels known from radioactive-decay work were not fully successful.

PACS. 23.20.-g Electromagnetic transitions – 23.20.Nx Internal conversion – 25.70.Gh Compound nucleus – 27.90.+b $220 \leq A$

1 Introduction

The nucleus ^{227}Th is located at the perimeter of a mass region - centered around ^{225}Ac - where both experimental and theoretical evidence suggests reflection-asymmetric nuclear shapes [1]. Due to its transitional character this nucleus constitutes one of the best cases for the coexistence of symmetric and reflection-asymmetric shapes, leading to the prediction of simple rotational bands for some orbits and parity-doublet bands for others [2]. To verify this interesting phenomenon it is necessary to identify many rotational bands to high spins and to study their γ -decay to decide on the existence or absence of enhanced E1 transitions between parity-doublet bands which are the fingerprints for reflection-asymmetric shapes. This goal can only be achieved by in-beam measurements of γ -rays following compound reactions which are difficult to perform in the actinides due to the overwhelming fission cross sections and the limited number of available targets. The best case for such investigations in the light actinides is ^{227}Th which can be studied in the $^{226}\text{Ra}(\alpha, 3n)$ reaction. We had started an investigation of this reaction some years ago by measuring $e^- - \gamma$ coincidences. This technique is particularly well suited for the in-beam study of actinides due to its potential to suppress the dominating γ -ray background from fission fragments [3]. This early investigation lead to the identification of two rotational bands in ^{227}Th [4,5], but it also demonstrated two problems:

(1) In order to fit the observed rotational bands into a level scheme of ^{227}Th it is necessary to have a knowledge of the low-lying levels in this nucleus from radioactive decay work, and to find an overlap of this scheme and the one from the in-beam work. At the time of our earlier work only two excited states were known in ^{227}Th , at 9.3 and 24.3 keV, which cannot be observed in the in-beam

work. We therefore started an investigation of the α -decay of ^{231}U to ^{227}Th [6] which resulted, together with the simultaneous study of the ^{227}Pa electron-capture decay by Liang et al. [7], in a detailed level scheme for ^{227}Th below $\sim 500\text{keV}$.

(2) The technique to measure $e^- - \gamma$ coincidences depends on the observation of sufficiently strong low-energy transitions with large conversion coefficients. In in-beam studies these are as a rule the lowest $\Delta I = 2$ E2 transitions between the strongly populated rotational bands, i.e. the bands close to the yrast line. In the present case the $e^- - \gamma$ measurements were limited to the two bands observed earlier, and the identification of further rotational bands required the measurement of $\gamma - \gamma$ coincidences. Fortunately, our measurements also indicated that the cross section for the $(\alpha, 3n)$ reaction was sufficiently large (several 100 mb) to allow such measurements. In the present report we present the results of our in-beam studies of ^{227}Th . Although we were not able to fit the observed rotational bands safely into a level scheme we feel that the data are extensive enough to justify a report in the hope to trigger further investigations of this interesting nucleus.

2 Experimental methods and results

A target of $\sim 300\mu\text{g}/\text{cm}^2$ of ^{226}Ra was bombarded with α -particles from the Bonn cyclotron. In a survey conversion electrons were measured at bombarding energies from 28 to 38 MeV yielding an optimum α -particle energy for the $(\alpha, 3n)$ reaction of $\sim 33\text{MeV}$. Most of the measurements described below were performed at this α -particle energy.

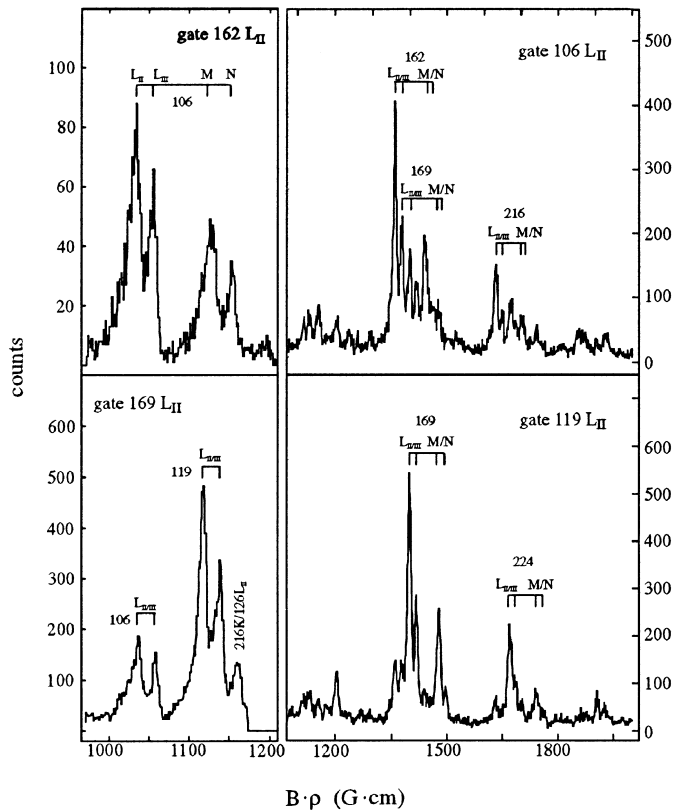


Fig. 1. Electron spectra in coincidence with L_{II} conversion electrons of the 106, 119, 162 and 169 keV transitions

2.1 $e^- - e^-$ coincidence measurements

The lowest transitions within the low-lying rotational bands in ^{227}Th are expected to be E2 transitions with energies below $\sim 150\text{keV}$. For such transitions internal conversion is the dominant decay mode requiring the measurement of conversion electrons. The measurements were performed using two iron-free orange spectrometers [8,9].

The strongest lines observed in the singles electron spectrum result from L-subshell conversion electrons of 106, 119, 162 and 169 keV E2 transitions. Electron spectra measured in coincidence with the L_{II} conversion electrons of these transitions are shown in Fig. 1. These data show that two rotational bands are strongly populated and decay by intraband E2 transitions with energies of 106, 162, 216 keV and 119, 169, 224 keV, respectively (in the following denoted as band 1 and band 2, see Fig. 10). None of these lines is present in the decay scheme known from radioactive decay work.

In an attempt to find the missing link between the two rotational sequences and the known level scheme we measured the low-energy electron-spectrum in coincidence with the 106 and 119 keV L_{II} conversion electrons. These measurements are restricted in our setup to electron energies above $\sim 40\text{keV}$ due to the overwhelming background from δ -electrons at lower energies. The resulting spectra, shown in Fig. 2, contain lines which can be interpreted as

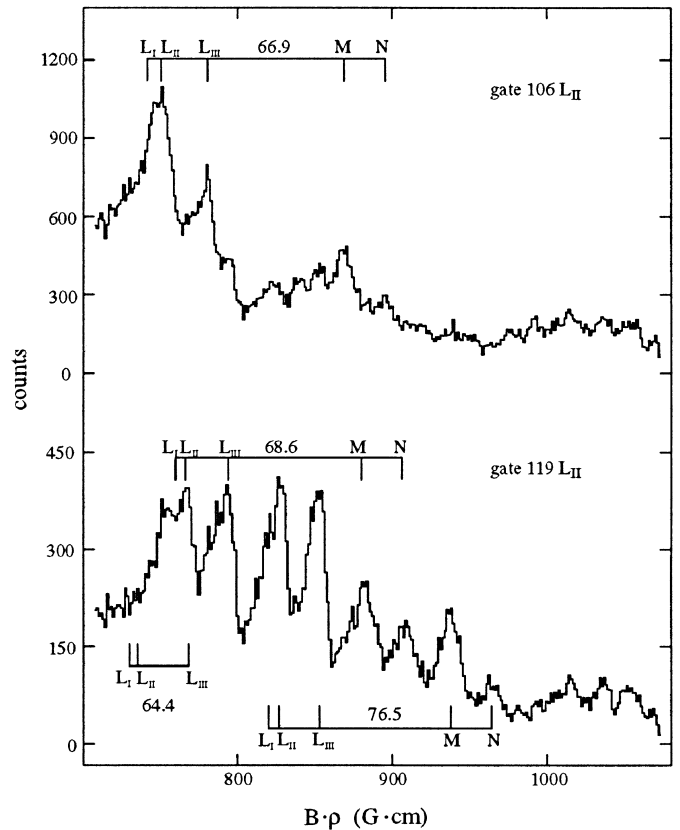


Fig. 2. Low-energy electron spectra in coincidence with L_{II} conversion electrons of 106 and 119 keV transitions

L and M-lines of 66.9, 68.6 and 76.5 keV E2 transitions. These possible transitions will play a crucial role in our attempt to place the rotational bands observed in the in-beam work into the level scheme of ^{227}Th (see Sect. 3.3).

2.2 $e^- - \gamma$ coincidence measurements

For the measurement of $e^- - \gamma$ coincidences one of the orange spectrometers was replaced by Ge detectors. Two arrangements were used, consisting of one LEPS detector and four Compton-suppressed detectors with $\sim 30\%$ efficiency, respectively [9]. The γ -ray spectra measured with the LEPS detector in coincidence with L_{II} conversion electrons of the 106 and 119 keV transitions are shown in Fig. 3. It is noted that the lines marked 64.8 keV (106 L_{II} gate) and 64.4 keV (119 L_{II} gate) are established to be different lines due to the good energy resolution of the LEPS detector ($\sim 500\text{eV}$ at 65 keV). The 64.4 keV line, as well as the 28.6 and 37.9 keV lines also observed in coincidence with the 119 keV transition, are the only lines measured in the in-beam work which are also observed in the radioactivity work, and interpreted there as E1 transitions from the lowest members of a $K^\pi = 1/2^-$ band with its bandhead at 37.9 keV to the $K^\pi = 1/2^+$ ground band [6]. This constitutes the second crucial evidence for the fit of the in-beam data into the level scheme of ^{227}Th . Finally, the observed γ -ray intensities of the lines marked in

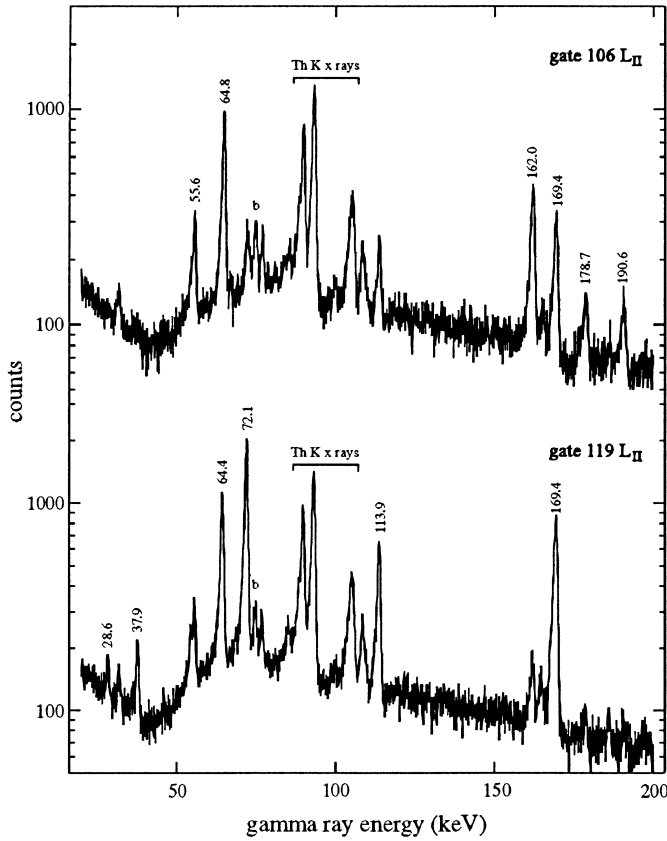


Fig. 3. Low-energy γ -ray spectra in coincidence with L_{II} conversion electrons of the 106 and 119 keV transitions. Background peaks are labeled by a 'b'

Fig. 3 by their energies up to the 113.9 keV line establish E1 multipolarity for these transitions.

Additional γ -ray spectra were measured with the LEPS detector in coincidence with conversion electrons of several of the low-energy peaks shown in Fig. 2. The results of these measurements are summarized in Table 1.

The γ -ray spectra measured with the four-detector set-up in coincidence with L_{II} conversion electrons of the 106, 119, 162 and 169 keV transitions are shown in Figs. 4 and 5. Many of the prominent lines can be assigned to the $\Delta I = 2$ intraband E2 transitions within bands 1 and 2. There are, however, a number of additional strong lines, for which no conversion-electrons are observed in the corresponding electron spectra (Fig. 1), and which can therefore be assigned as E1 transitions. The strongest ones are marked by their energies: 178.7, 190.6 and 209.4 keV lines in Fig. 4 and 113.9, 169.4 (gate 169 L_{II}), 211.1 and 239.8 keV lines in Fig. 5. For the placement of these E1 transitions in the decay scheme it was necessary to measure $\gamma - \gamma$ coincidences.

2.3 $\gamma - \gamma$ coincidence measurements

Gamma-gamma coincidences were measured using an array of five Compton-suppressed Ge detectors placed on

Table 1. Gamma rays in coincidence with low-energy conversion electrons (energies in keV)

E_{e^-}	interpretation E_γ shell	E_γ of coincident γ -rays ^a
47.2	66.9 L_{II}	64.9, 72.2, 85.3 ^w , 114.0 ^w , 169.6
50.6	L_{III}	64.9, 72.3, 114.1 ^w , 119.3 ^w , 169.7
48.9	68.6 L_{II}	54.2 ^w , 55.6 ^{vw} , 64.9, 72.2, 114.0 ^w , 119.1 ^{vw} , 169.6
52.3	L_{III}	64.1 ^w , 64.9, 71.0 ^w , 72.1, 114.0 ^{vw} , 169.3
64.1	M	54.4 ^{vw} , 56.0 ^{vw} , 65.0, 72.3, 114.2 ^w , 119.4 ^{vw} , 126.4 ^{vw} , 169.7
56.8	76.5 L_{II}	54.3 ^w , 55.8 ^{vw} , 64.6, 72.3 ^w , 114.1 ^w , 119.2 ^w , 169.5
60.1	L_{III}	54.1 ^w , 55.5 ^{vw} , 64.5, 72.1 ^w , 114.2, 119.4, 169.5
72.0	M	54.3 ^w , 55.8 ^w , 64.5, 72.2 ^w , 114.1 ^w , 119.2 ^w , 169.6

^a) γ -rays marked by $w(vw)$ are weak (very weak)

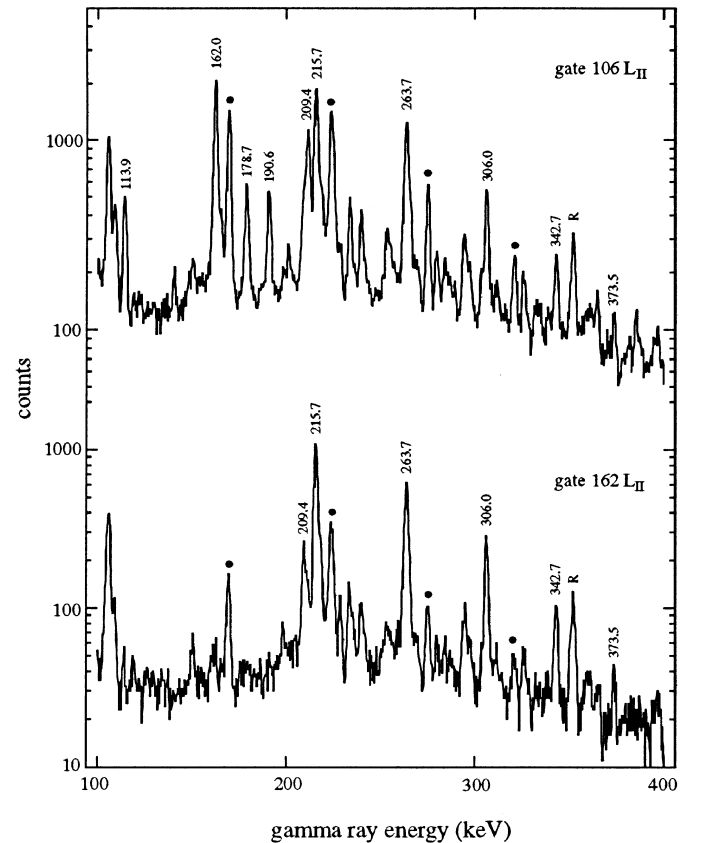


Fig. 4. Gamma-ray spectra in coincidence with L_{II} conversion electrons of the 106 and 162 keV transitions. The transitions within band 2 (see Fig. 10) are marked by dots. The 'R' indicates peaks arising from the radioactivity of the ^{226}Ra target

the faces of a cube, with the beam directed through the diagonal of the four detectors located in the horizontal plane. The coincidences were recorded in list-mode tech-

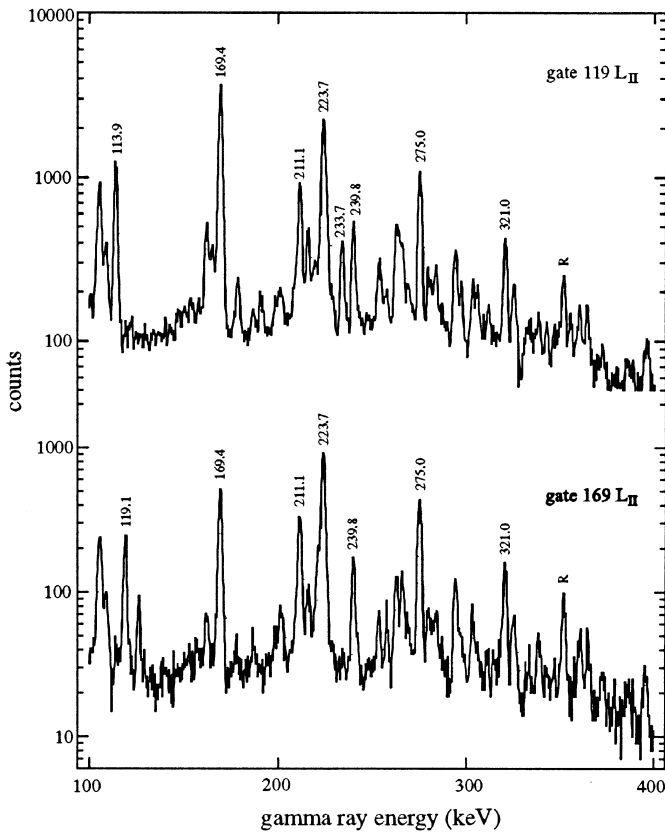


Fig. 5. Gamma-ray spectra in coincidence with L_{II} conversion electrons of the 119 and 169 keV transitions. The 'R' indicates peaks arising from the target radioactivity

nique, and a coincidence matrix was created and analysed with the Radford package.

Some selected coincidence spectra are shown in Figs. 6 to 9 to illustrate the assignments leading to the level scheme discussed below. The spectra in coincidence with higher-lying intraband E2 transitions of bands 1 and 2 are shown in Figs. 6 and 7, respectively. These spectra illustrate the E1 transitions feeding from two additional bands (band 3 and band 4) into the bands 1 and 2.

The γ -ray spectra in coincidence with the 114 and 179 keV lines are shown in Fig. 8. These two gate-lines are interpreted as depopulating the lowest observed level of band 4, which is directly populated by the intraband 224.7 transition and the 233.7 keV transition from the lowest observed level of band 5. Finally, the γ -ray spectra in coincidence with the 233.7 keV transition depopulating band 5 and the lowest observed intraband transition within this band are shown in Fig. 9 illustrating the double assignment of the 254 keV line in the level scheme leading to band 6.

3 Discussion

In this section we will present the level structure obtained from the in-beam study and discuss some of the considerations leading to this structure. Some properties of the

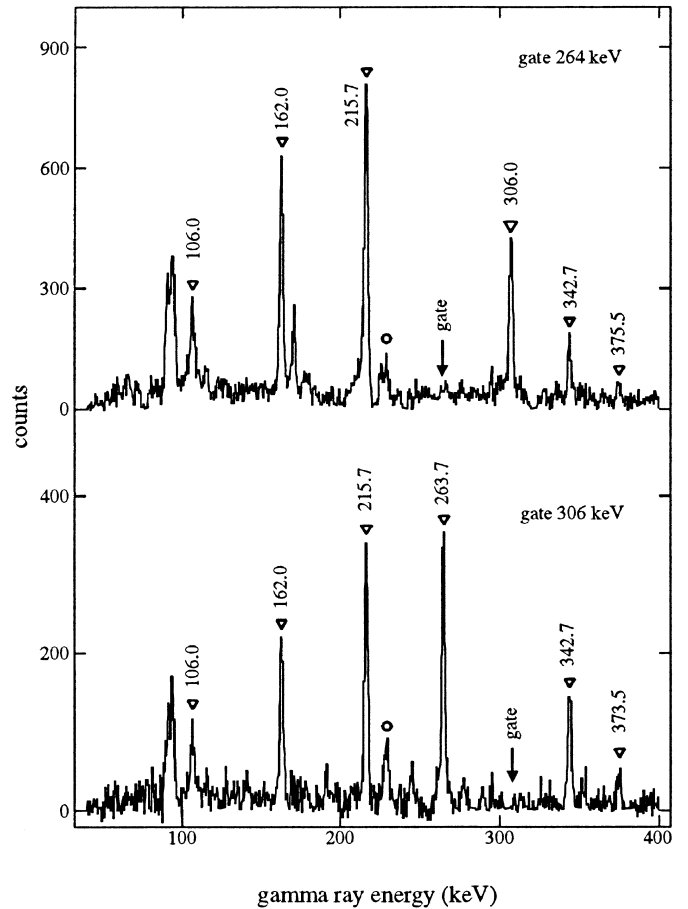


Fig. 6. Gamma-gamma coincidence spectra with gates on the 264 and 306 keV lines. The intraband E2 and interband E1 transitions are marked by triangles and circles, respectively

resulting rotational bands will be discussed in a second subsection. Finally, we will present a possibility to fit the in-beam level structure into the level scheme known from radioactivity studies and discuss the difficulties encountered in this attempt.

3.1 Rotational bands in ^{227}Th

The level structure of ^{227}Th derived from the present work is shown in Fig. 10. We will briefly discuss each of the six rotational bands.

Bands 1 and 2: These two bands are most strongly populated in the $(\alpha,3n)$ reaction with $\frac{I_{tot}(106\text{ keV})}{I_{tot}(119\text{ keV})} = 1.54 \pm 0.15$. They were previously identified by Schüler et al. [4,5], and they form the backbone of the level structure derived from the in-beam work. The rotational sequence within the two bands is based on the observation of a series of coincident E2 transitions - E2 multipolarity is established for the lowest five and four transitions in band 1 and 2, respectively, from the L-subshell conversion-electron intensities - which are assumed to be stretched $I \rightarrow I - 2$ transitions.

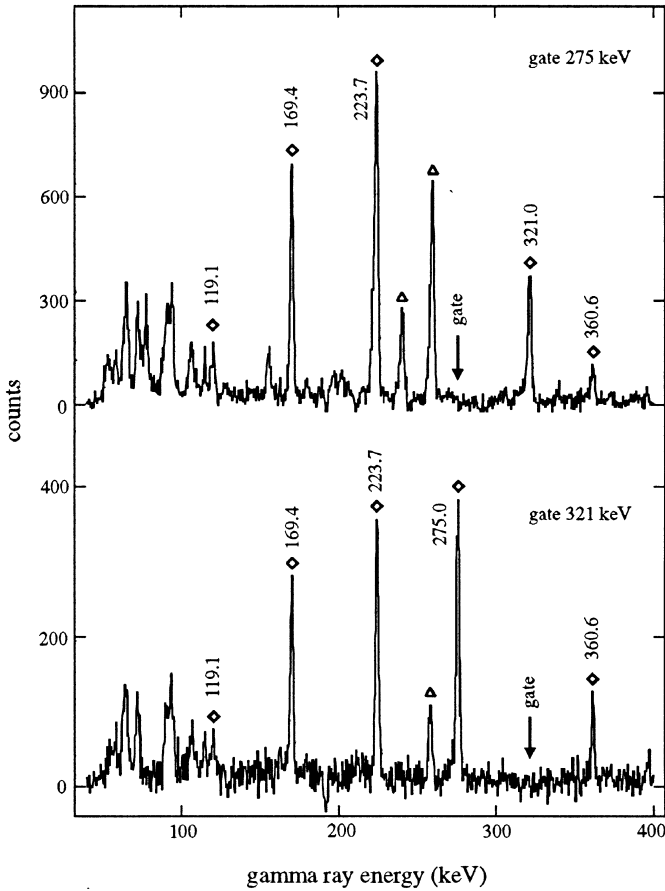


Fig. 7. Gamma-gamma coincidence spectra with gates on the 275 and 321 keV lines. The diamonds and triangles mark intraband E2 and interband E1 transitions, respectively

The relative location of the two bands is indicated by the fact, that the transitions within band 2 are observed fairly strongly in the coincidence spectra with gates on the lowest transitions within band 1, whereas the opposite coincidences (band 1 in gates of band 2) are much weaker (see Figs. 3 to 5). The quantitative assignment shown in Fig. 10 is based on the observation of the 64.8, 113.9 and 178.7 keV γ -rays in coincidence with the 106 keV transition, and the 54.3 and 72.2 keV γ -rays in coincidence with the 162 L_{II} conversion electrons.

Bands 3 and 4: A few strong γ -ray lines are observed in the $\gamma - \gamma$ coincidence spectra for which no K conversion-electrons are seen in the electron spectrum. This establishes E1 multipolarity for these transitions, and we assign them to stretched E1 transitions from two new bands to band 1 (band 3) and band 2 (band 4) (for the doubly-placed 169 keV γ -rays we obtain from the $\gamma - \gamma$ and $e^- - \gamma$ coincidence spectra an intensity ratio of $\frac{I_\gamma(169\text{keV},E1)}{I_\gamma(169\text{keV},E2)} = 0.7 \pm 0.1$). The placement of these two additional bands in the level scheme is supported by the observation of weak intraband transitions as shown in the level scheme of Fig. 10.

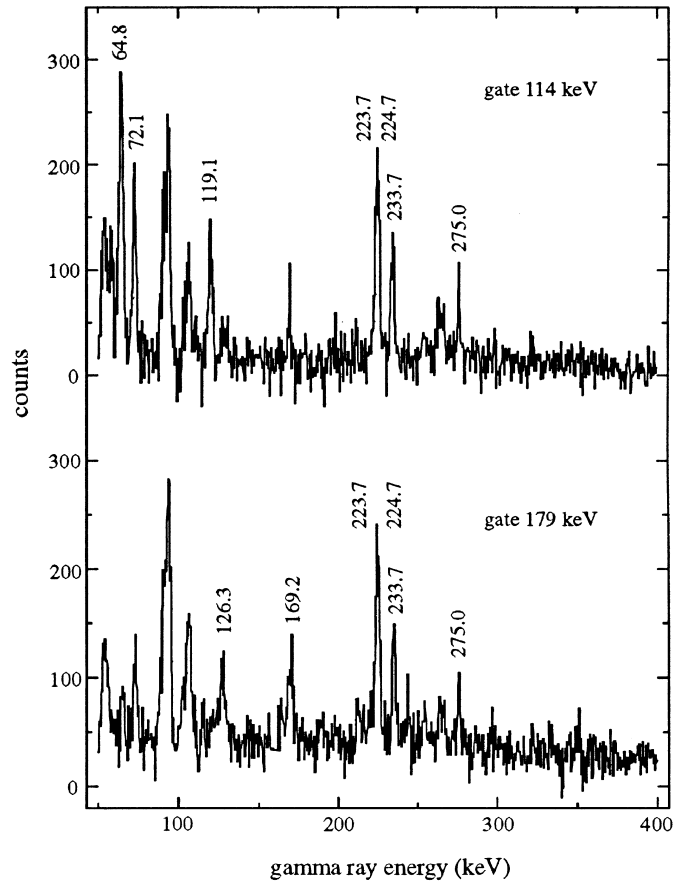


Fig. 8. Gamma-gamma coincidence spectra with gates on the 114 and 179 keV lines

Bands 5 and 6: Several additional weak γ -ray lines are observed in the coincidence spectra (see e.g. Figs. 8 and 9) which suggest level sequences shown as band 5 and band 6 in Fig. 10. While band 5 seems to be fairly well established by the available energy loops, band 6 is only tentative.

3.2 Properties of the rotational bands

In Fig. 11 we plotted the experimental results of the quantity $(2I+1)/E_\gamma((I+1) \rightarrow (I-1))$ versus spin I for bands 1 and 2 in ^{227}Th and the ground bands of the neighbouring isotopes ^{226}Th and ^{228}Th . For the two bands in ^{227}Th we have assumed the spins given in Sect. 3.3 below. In the simplest rotational model the plotted quantity is given for bands with $K \neq 1/2$ and for the energy-favoured signature branches of $K = 1/2$ bands by the relation

$$\frac{2I+1}{E_\gamma((I+1) \rightarrow (I-1))} = \frac{J}{\hbar^2} \cdot \frac{2I+1}{2I+1 - |a| \cdot \delta(K, 1/2)}$$

where J is the moment of inertia and a is the decoupling parameter of the $K = 1/2$ band. The increase of the plotted quantity for the two bands in ^{227}Th at low spins can be accounted for by assuming these bands to be the energy-favoured branches of $K = 1/2$ bands with $|a| \approx 4$. At high

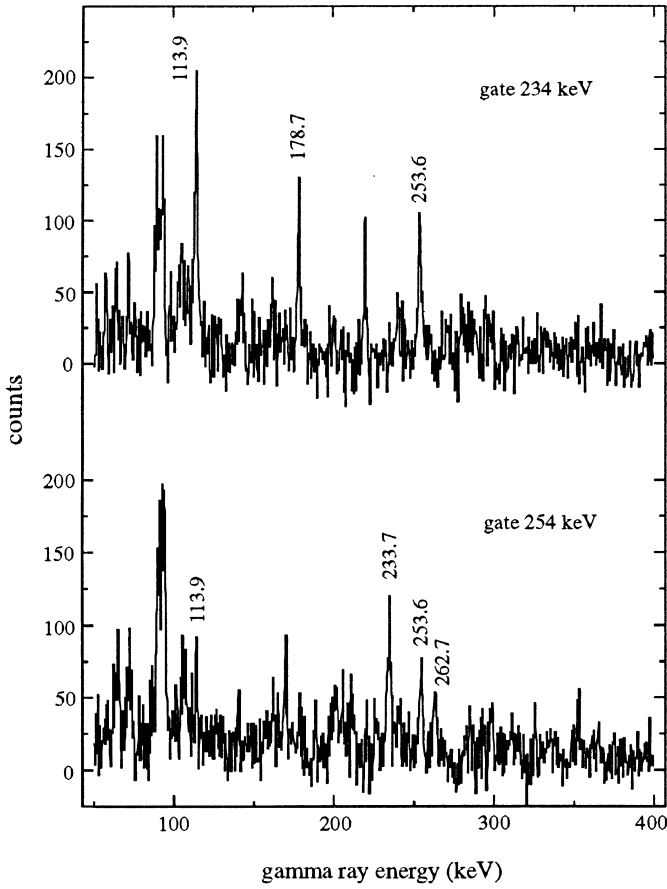


Fig. 9. Gamma-gamma coincidence spectra with gates on the 234 and 254 keV lines

spins the decoupling can be neglected and the experimental data indicate an increase of the moment of inertia for the bands in ^{227}Th compared to that of the even-even core, by $\sim 15\%$. This is a general feature observed for deformed nuclei attributed to the modification of the even-even core by the odd particle (see e.g. [10] pp. 249ff).

As discussed above we interpret the observed γ -rays as stretched interband E1- and intraband E2-transitions. In a few cases both the E1 and E2 transitions depopulating a given level are observed allowing to determine $B(E1)/B(E2)$ ratios. If the two $\Delta I = 2$ sequences connected by the E1 transitions are the members of parity-doublet bands in an octupole-deformed nucleus, the E1 and E2 transition matrix-elements can be interpreted in terms of intrinsic electric dipole (D_0) and quadrupole (Q_0) moments [1] yielding

$$\frac{B(E1, I \rightarrow (I-1))}{B(E2, I \rightarrow (I-2))} = \frac{16}{5} \frac{(I-1/2)(I-1)}{(I-K-1)(I+K-1)} \left(\frac{D_0}{Q_0}\right)^2$$

The experimental $B(E1)/B(E2)$ ratios are presented in Table 2. The values given in the last column can be compared with the ratio $D_0/Q_0 \approx 2.6 \cdot 10^{-4} \text{fm}^{-1}$ obtained from an interpolation of the corresponding ratios for the even-even neighbours [11]. The observed values are

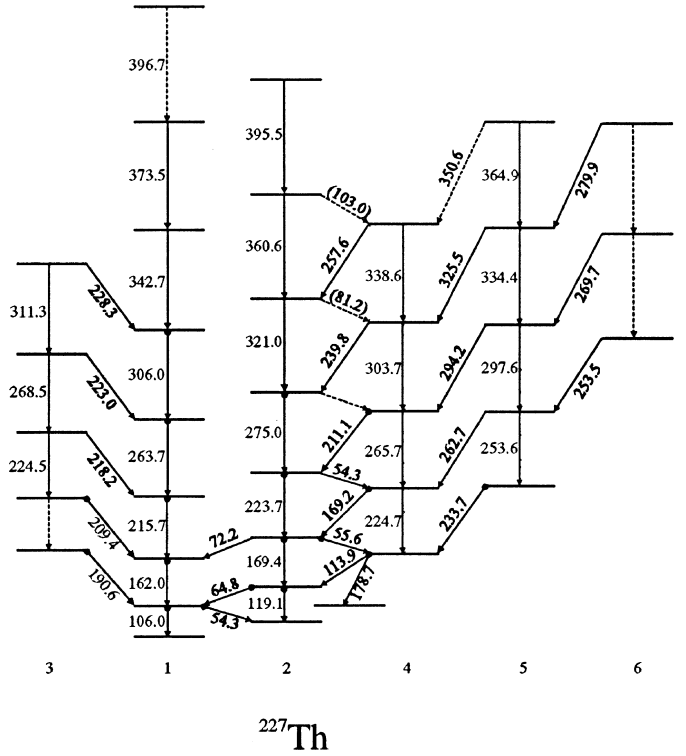


Fig. 10. Level structure of ^{227}Th observed in the $^{226}\text{Ra}(\alpha, 3n)^{227}\text{Th}$ reaction

Table 2. $B(E1)/B(E2)$ ratios

band nr.	$E_\gamma(E1)$ (keV)	$E_\gamma(E2)$ (keV)	$I_\gamma(E1)/I_\gamma(E2)$	$\sqrt{\frac{5}{16} \cdot \frac{B(E1)}{B(E2)}} (10^{-4} \cdot \text{fm}^{-1})$
2	64.8	119.1	1.5 ± 0.3	1.8 ± 0.2
	72.2	169.4	0.16 ± 0.03	1.2 ± 0.1
4	211.1	265.7	1.3 ± 0.2	2.1 ± 0.2
	239.8	303.7	1.9 ± 0.3	2.9 ± 0.2
5	262.7	253.6	1.1 ± 0.2	1.2 ± 0.1

of this magnitude indicating that octupole correlations are important in ^{227}Th .

3.3 Attempt to introduce the rotational bands into a level scheme

As emphasized above three γ -rays with energies of 28.6, 37.9 and 64.4 keV are observed in coincidence with the 119 keV transition in the $^{226}\text{Ra}(\alpha, 3n)^{227}\text{Th}$ reaction, which are known from radioactivity work and assigned to the level scheme of ^{227}Th . The $e^- - e^-$ - and $e^- - \gamma$ -coincidences discussed in section 2 suggest the placement of the 119 keV transition in the level scheme as shown in Fig. 12. The E1/E2 branching of the $11/2^-$ level would be consistent with the proposed interpretation: with $D_0/Q_0 = 2.6 \cdot 10^{-4} \text{fm}^{-1}$ the $11/2^-$ level is predicted

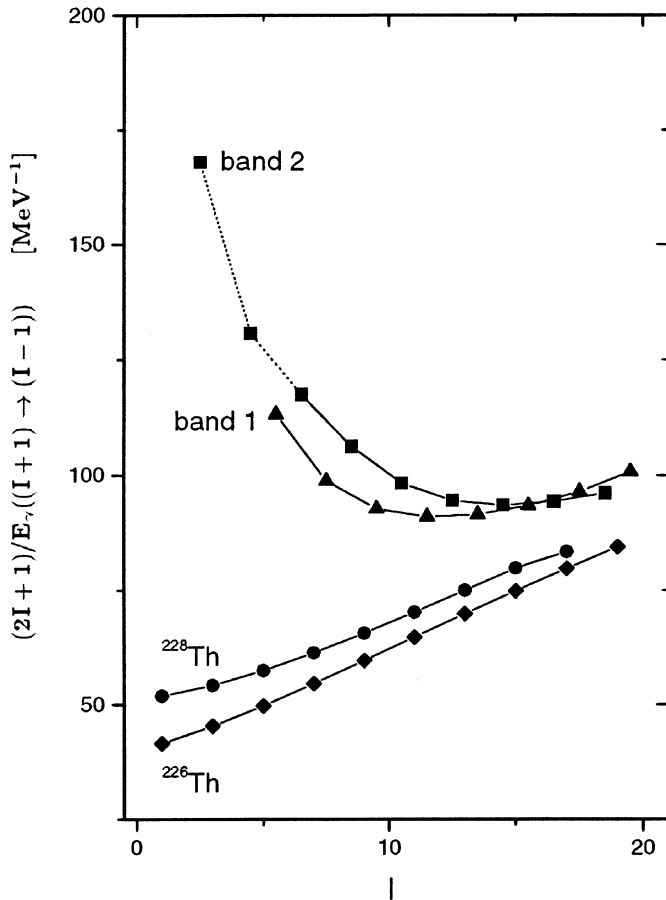


Fig. 11. Moments of inertia of the ground bands in ^{226}Th and ^{228}Th and the bands 1 and 2 in ^{227}Th as a function of spin (see text). The two lowest data points connected with the dotted line are obtained from the radioactivity work (see Fig. 12)

to decay to 45 % by the 72.1 keV γ -ray and to 41 % by the 76.5 keV conversion electrons. Unfortunately, the proposed level scheme leads to serious problems with the positive-parity levels, in particular in connection with the placement of the 106 keV E2 transition:

(1) The proposed scheme would lead to two closely-spaced $9/2^+$ levels which would be difficult to explain on the basis of the known level structure. Moreover, the rotational structure of band 1 discussed above suggests that this band constitutes the high-spin part of the ground band. In this case one would expect that the 98.4 keV $9/2^+$ level decays by a 89.1 keV E2 transition to the 9.3 keV $5/2^+$ level, but such a transition is not observed in our $e^- - e^-$ coincidence measurements.

(2) The $e^- - e^-$ coincidences indicate that the 106 keV transition is in coincidence with a 66.9 keV E2 transition. A transition with this energy is known to depopulate a 76.2 keV level. This lead to the suggestion of a depopulation of the 98.4 keV level by an unobserved 22.2 keV transition to this latter level as indicated in Fig. 12. However, in the γ -ray spectra in coincidence with the proposed 66.9 keV L_{II} and L_{III} conversion electrons there is no indica-

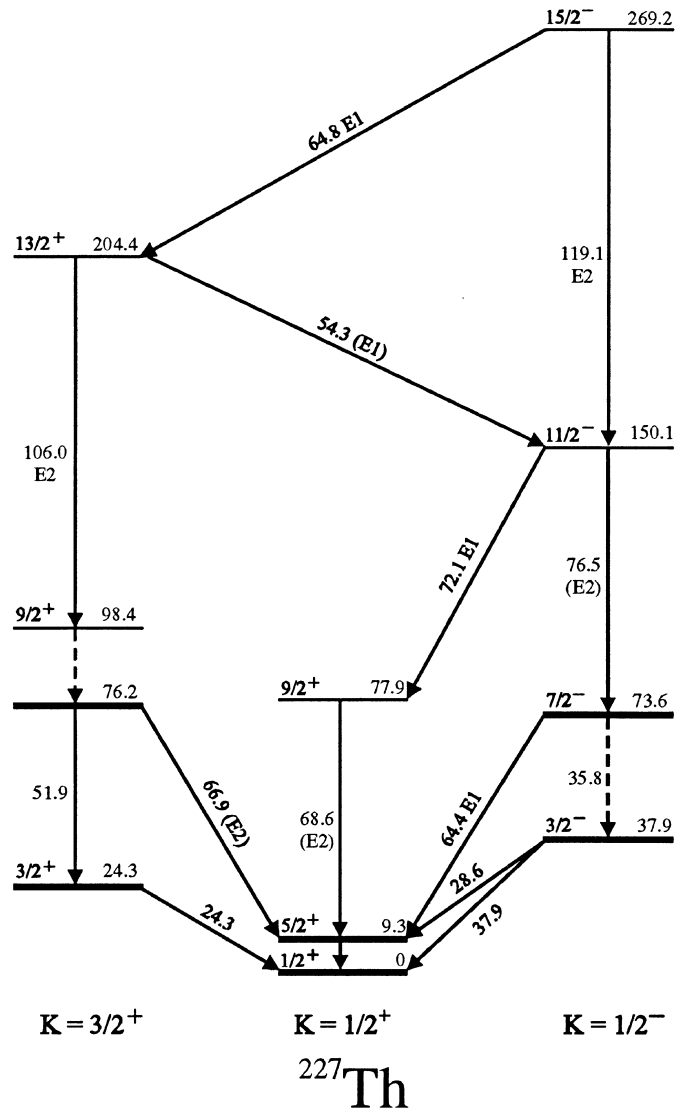


Fig. 12. Possible placements of the bands 1 and 2 into a level scheme of ^{227}Th . The levels known from the radioactive decay work are represented by thick lines

tion of the 162 keV γ -rays expected from the E2 transition above the 106 keV transition in band 1.

We have therefore to conclude that we do not yet understand the placement of the rotational bands observed in the $(\alpha, 3n)$ reaction in the level scheme. While the insertion of band 2 seems quite convincing, it leads to consequences for band 1 which are difficult to reconcile with experimental observations.

In closing this section we would like to mention that a number of additional weak lines are observed in the $\gamma - \gamma$ coincidence spectra which could not be fitted into the level scheme due to the limited statistics of our $\gamma - \gamma$ coincidences [12]. One γ -ray which could be of particular significance has an energy of 126.3(2) keV. This energy agrees with the energy difference of the 77.9 keV $9/2^+$ and 204.4 keV $13/2^+$ levels proposed in Fig. 12. However, the 126 keV γ -ray is not in coincidence with the 106 and

119 keV transitions but in clear coincidence with the 169 keV $E2$ transition (see Figs. 4 and 5).

4 Conclusion

The present work has shown that it is possible to study the nucleus ^{227}Th in detail in the $^{226}\text{Ra}(\alpha,3n)$ reaction. From conversion-electron and γ -ray coincidence measurements six rotational bands could be identified. Unfortunately, it has not yet been possible to introduce these bands into a level scheme, although detailed information on the low-lying levels of ^{227}Th is available from radioactive decay work.

Crucial further information could be obtained from an improved $\gamma - \gamma$ coincidence measurement. In the present work the $\gamma - \gamma$ coincidences were recorded using a setup with 5 Compton-suppressed Ge detectors, and thus only double coincidences could be obtained with moderate statistics ($4 \cdot 10^7$ coincidences). A significant improvement would be possible using one of the new generation of Ge detector arrays, allowing to obtain orders of magnitude better statistics for the double coincidences as well as the analysis of triple coincidences. Such data would hopefully enable the incorporation of the in-beam data into a level scheme. In addition it would enable the extension of the observed rotational bands to higher spins and the determination of more accurate data on the $B(E1)/B(E2)$ ratios which provide the fingerprints for octupole correlations.

This work was partly funded by DFG grants Bo 1109/1 (J.d.B.) and Gu 179/3-4 (J.M., J.G., C.G., U.M., T.W.).

References

1. Butler, P.A., Nazarewicz, W.: Rev. Mod. Phys. 68, 349 (1996)
2. Cwiok, S., Nazarewicz, W.: Phys. Lett. B 224, 5 (1989) and Nucl. Phys. A529, 95 (1991)
3. Janssens, R.V.F., Jansen, J.F.W., van Klinken, J., Steendam, S.P., Lukasiak, J., Venema, W.Z., Wempe, W.E.M.P.E.: Nucl. Instr. Meth. 187, 635 (1981)
4. Schüler, P.: PhD thesis, University of Bonn (1986)
5. Ackermann, B., Grafen, V., Günther, C., Euler, K., Marten-Tölle, M., Tölle, R., Zeyen, P.: Annual Report 1985 - 87, ISKP, University of Bonn (1987), p. 102
6. Müller, U., Sevenich, P., Freitag, K., Günther, C., Herzog, P., Jones, G.D., Kliem, C., Manns, J., Weber, T., Will, B., and the ISOLDE Collaboration: Phys. Rev. C 55, 2267 (1997)
7. Liang, C.F., Paris, P., Sheline, R.K., Nosek, D., Kvasil, J.: Phys. Rev. C 51, 1199 (1995)
8. Kölschbach, V., Schüler, P., Hardt, K., Rosendaal, D., Günther, C., Euler, K., Tölle, R., Marten-Tölle, M., Zeyen, P.: Nucl. Phys. A439, 189 (1985)
9. Hughes, J.R., Tölle, R., deBoer, J., Butler, P.A., Günther, C., Grafen, V., Gollwitzer, N., Holliday, V.E., Jones, G.D., Lauterbach, C., Marten-Tölle, M., Mullins, S.M., Poynter, R.J., Simon, R.S., Singh, N., Tanner, R.J., Wadsworth, R., Watson, D.L., White, C.A.: Nucl. Phys. A512, 275 (1990)
10. Bohr, A., Mottelson, B.R.: Nuclear structure, Vol.II. Reading, Mass.: Benjamin (1975)
11. Ackermann, B., Baltzer, H., Ensel, C., Freitag, K., Grafen, V., Günther, C., Herzog, P., Manns, J., Marten-Tölle, M., Müller, U., Prinz, J., Romanski, I., Tölle, R., deBoer, J., Gollwitzer, N., Maier, H.J.: Nucl. Phys. A559, 61 (1993)
12. Manns, J.: PhD thesis, University of Bonn (1996)